

# 1 Preparation of TFC Membranes Supported with Electrospun Nanofibers 2 for Desalination by Forward Osmosis

3 Mustafa Al-Furaiji<sup>1,\*</sup>, Mohammed Kadhom<sup>2</sup>, Khairi Kalash<sup>1</sup>, Basma Waisi<sup>3</sup>, Noor Albayati<sup>4</sup>

4 <sup>1</sup> Environment and Water Directorate, Ministry of Science and Technology, Baghdad, Iraq

5 <sup>2</sup> Department of Environment, College of Energy and Environmental Sciences, Alkarkh University of Science, Baghdad, Iraq

6 <sup>3</sup> Department of Chemical Engineering, College of Engineering, University of Baghdad, Baghdad, Iraq

7 <sup>4</sup> Department of Science, College of Basic Education, University of Wasit, Azizia, Wasit, Iraq

8 Corresponding Author: email: [alfuraiji79@gmail.com](mailto:alfuraiji79@gmail.com); phone: +964-7736-792-156

## 9 Abstract

10 Forward osmosis (FO) process has been considered as a viable option for water desalination in  
11 comparison to the traditional processes like reverse osmosis, regarding energy consumption and  
12 economical operation. In this work, polyacrylonitrile (PAN) nanofiber support layer was prepared using  
13 electrospinning process as a modern method. Then, an interfacial polymerization reaction between m-  
14 phenylenediamine (MPD) and trimesoyl chloride (TMC) was carried out to generate a polyamide  
15 selective thin film composite (TFC) membrane on the support layer. The TFC membrane was tested in  
16 FO mode (feed solution facing the active layer) using the standard methodology and compared to a  
17 commercially available cellulose triacetate membrane (CTA). The synthesized membrane showed a high  
18 performance in terms of water flux ( $16 \text{ Lm}^{-2}\text{h}^{-1}$ ) but traded the salt rejection ( $4 \text{ gm}^{-2}\text{h}^{-1}$ ) comparing with  
19 the commercially CTA membrane (water flux=  $13 \text{ Lm}^{-2}\text{h}^{-1}$  and salt rejection=  $3 \text{ gm}^{-2}\text{h}^{-1}$ ) at no applied  
20 pressure and room temperature. Scanning electron microscopy (SEM), contact angle, mechanical  
21 properties, porosity, and performance characterizations were conducted to examine the membrane.

22

23 **Keywords: Forward Osmosis; TFC membrane; Desalination; Nanofibers; Electrospinning**

24

## 25        **1. Introduction**

26 Forward osmosis is an osmotically-driven membrane process that uses the difference in osmotic pressure  
27 between the feed solution and a highly concentrated solution (called draw solution) to drive the pure water  
28 from feed solution through the membrane to the draw solution. The FO process has many advantages over  
29 other types of filtration processes, such as its low or no trans-pressure, very high rejection for various  
30 contaminants, low membrane fouling tendency, and easy building and operating system. The used  
31 system is very simple and membrane support is less of a problem (Al-Furaiji et al., 2018; Cath et al.,  
32 2006).

33 One of the crucial aspects of developing the FO process is making a suitable membrane for this process.  
34 The ideal membrane has to be highly porous, thin, owning good mechanical properties, and provides high  
35 rejection of salts and impurities (Ang et al., 2019). Thin-film composite (TFC) membranes have been  
36 widely used in reverse osmosis studies and proven to have excellent performance in desalination (Kadhom  
37 et al., 2016; Kadhom and Deng, 2019). However, recently TFC membranes have attracted more attention  
38 in FO applications.

39 Commonly, the TFC membranes consist of two layers: a thin selective film that permits water molecules  
40 to pass through but prevents salts and other contaminations, and a support layer that provides the required  
41 mechanical backing (Ren and McCutcheon, 2014). The selective thin layer is typically prepared by the  
42 interfacial polymerization reaction of *m*-phenylenediamine aqueous solution and 1,3,5-  
43 Benzenetricarbonyl trichloride, which is familiarly called trimesoyl chloride, organic solution on the  
44 support layer. The support sheet is conventionally prepared by the phase inversion casting method. Here,  
45 we adopted an emerging technology, electrospinning, to make the support layer. Electrospinning has some  
46 advantages over the traditional phase inversion technique that include producing highly porous layer and  
47 generating sub-micron fibers with highly controllable properties (Waisi et al., 2019). These properties  
48 have led to introduce these nanofiber sheets as promising alternatives for the conventional FO  
49 membrane's support layers. Bui and McCutcheon 2013 investigated blending two kinds of polymer (i.e.  
50 PAN and cellulose acetate) to make hydrophilic nanofibers for FO applications (Bui and McCutcheon,  
51 2013). Huang and McCutcheon 2014 used Nylon 6,6 electrospun nanofibers as support for TFC FO

52 membranes (Huang and McCutcheon, 2014). Chowdhury et al. 2016 prepared and tested a TFC  
53 membrane supported with commercial polyethersulfone (PES) nanofiber membranes (Chowdhury et al.,  
54 2017). All these electrospun nanofibers based TFC membrane showed excellent performance over the  
55 commercial FO membranes.

56 In this work, a thin-film composite polyamide membrane was synthesized by reacting MPD and TMC on  
57 the electrospun PAN nanofibers support layer and utilized in the forward osmosis process. **The**  
58 **electrospun PAN nanofibers were prepared using a home-made electrospinning setup that was fabricated**  
59 **from locally available parts; highly porous and highly efficient nanofibers were produced using a very**  
60 **low-cost method.** The membranes prepared in this study were mainly characterized by SEM and contact  
61 angle to investigate the impact of the highly porous support layer, in addition to other tests. FO  
62 experiments were carried out using a custom-built setup that utilize sodium chloride as a draw solution  
63 for the process.

## 64 **2. Materials and Methods**

### 65 **2.1. Materials**

66 Polyacrylonitrile (PAN) of an average molecular weight of 150,000 was purchased from Macklin,  
67 Shanghai, China. N, N-dimethylformamide (DMF), and Isooctane were obtained from Fluka Chemie AG,  
68 Buchs, Switzerland. The interfacial polymerization raw materials (*m*-phenylenediamine (>99%) and  
69 trimesoyl chloride (98%)) were ordered from Merck. Sodium chloride (NaCl) was purchased from  
70 Thomas Baker, India. Polyethersulfone (PES) of M.wt. = 150,000 was purchased from Macklin  
71 (Shanghai, China).

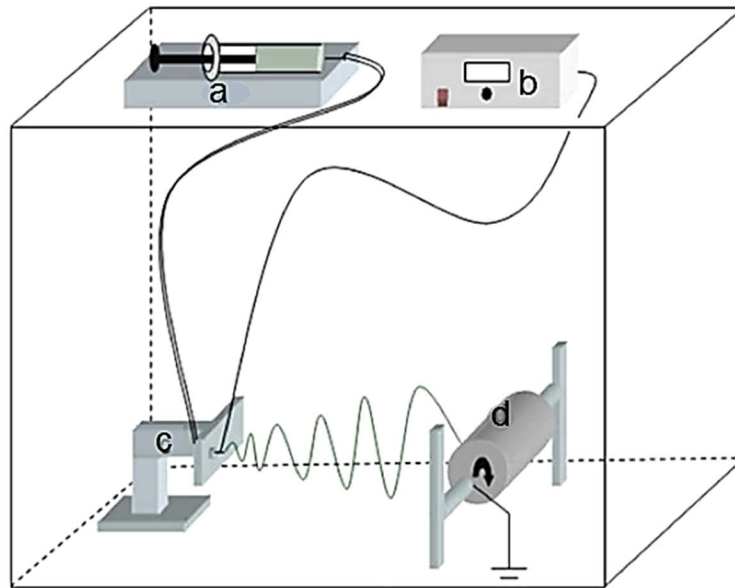
72 The control membrane used in this work was CTA (cellulose triacetate) forward osmosis membrane. This  
73 membrane was provided by Hydration Technology Innovations (HTI) Water Technology (Albany, OR)  
74 and been widely applied for a number of FO applications such as seawater desalination (Linares et al.,  
75 2017), wastewater treatment (Al-Furaiji et al., 2019), and advanced life support systems (Cath et al.,  
76 2005). Properties and images of the membrane can be found elsewhere (McCutcheon et al., 2005).

## 2.2. PAN nanofiber and PES support layers fabrication

PAN nanofibers were prepared using a custom-built electrospinning setup (Figure 1). The electrospinning setup contained a high voltage power supply, a syringe pump, and a rotating drum. Syringe pump was made from locally available materials. A grounded aluminum rotating drum, which served as a collector, was placed on a distance of 15 cm from the needle's tip, and an electrical potential was used at a voltage of 30 kV using the power supply device.

The solution of PAN in DMF was prepared by continuously stirring the polymer in the solvent for 24 h at 60°C. After obtaining the desired solution, it was left to cool and degas overnight at room temperature prior to electrospinning. The as-prepared polymeric solution was electrospun at a flow rate of 1 mL/h onto an aluminum foil which is peeled off before using the membrane in preparing the TFC membranes. Electrospinning was conducted at ambient temperature and humidity.

In order to compare the mechanical properties of the prepared support layer with a common support layer used for the same purpose, a polyethersulfone support sheet was prepared via the phase inversion phenomenon. 15% PES was dissolved in DMF by applying heat and stirring for 3 h until a colorless solution formed without any polymer residue. After maintaining the solution at 60 °C during heating, it was left to cool at room temperature overnight for degassing. The solution was extended on a glass plate via a home-made casting knife to a thickness of 130 μm and immersed in a water bath. The solution turned to a white sheet and separated from the glass in a few seconds. The sheet was rinsed with water three times before storing and use.



98

99 **Figure 1 A diagram of the custom-built Electrospinning setup, (a) syringe pump, (b) high voltage supply, (c)**  
 100 **transition stage, and (d) rotating collector.**

101

### 102 **2.3. Interfacial Polymerization to Make TFC Membrane.**

103 The TFC membranes were prepared via the interfacial polymerization reaction at the interface between  
 104 MPD aqueous solution and TMC organic solution. 2% of MPD was dissolved in DI water to prepare the  
 105 aqueous solution, while the organic solution was prepared by dissolving 0.15% of TMC in isooctane. The  
 106 IP reaction was conducted on the PAN support layer as follows: First, the as-spun PAN was mounted on  
 107 a glass plate and the MPD solution was poured on its top and kept in contact with the PAN support sheet  
 108 for 60 s (Kadhom et al., 2016). The excess of the solution was ejected using a squeegee ruler. Then, the  
 109 TMC solution was poured on the PAN sheet that contained the MPD active sites and kept in contact for  
 110 30 s. The resulting TFC membrane was then dried for 10 min at 60°C and stored in DI water prior to the  
 111 performance examination.

112

113

## 2.4. Membranes Characterizations

The Morphology analysis of the prepared membranes was determined using a Scanning Electron Microscope (SEM, VEGA3 - TESCAN, Czechoslovakia). The mechanical properties of the different membranes were obtained from the tensile tests in the air at 25 °C using an Instron microforce tester. A dynamic mechanical analysis (DMA) controlled force module was selected and a minimum of three strips (with a size of 40 mm x 5.5 mm) were tested from each type of membrane. The porosity of the membranes was estimated using the gravimetric method. The membrane was cut as disks with a diameter of 2.54 cm (1 in) and weighed ( $W_{dry}$ ). Isopropyl alcohol (IPA) was used as a wetting agent and the membrane weighed after immersed in IPA ( $W_{wet}$ ). The porosity ( $\varepsilon$ ) was calculated from the following equation:

$$\varepsilon = \frac{\left( \frac{W_{wet} - W_{dry}}{\rho_{IPA}} \right)}{V} \times 100\%$$

where  $\rho_{IPA}$  is the density of IPA and  $V$  is the total volume of the sample. Each membrane was tested at least three times. The membranes' wettability was studied by measuring the contact angle (Theta Lite TL-101 Thailand).

## 2.5. Forward osmosis performance tests

The FO tests were carried out using the experimental set-up illustrated in Figure 2. The installation consists of two tanks: one was specified for the feed solution, while the other was for the draw solution. Both solutions were pumped to the membrane cell using diaphragm pumps from Pure-water®. The membrane was installed in a custom-made cell with dimensions of 7.62 cm length, 2.54 cm width, and 0.3 cm depth. The selection of the feed and draw solutions was according to the standard methodology described by Cath et al. 2013. The DI water was used as a feed solution while 1 M NaCl solution was used as a draw solution. The water permeation flux was estimated as follows:

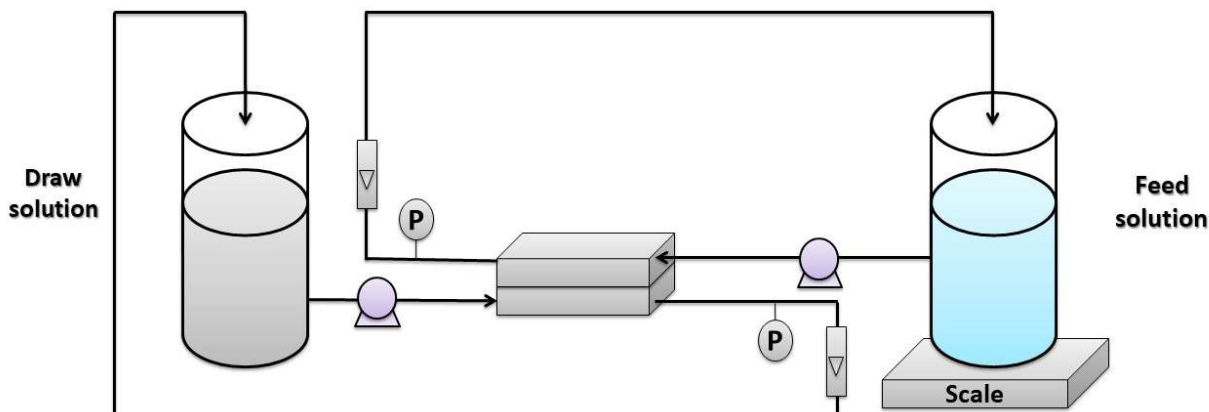
$$J_w = \frac{\Delta w}{\rho A t}$$

Where  $J_w$  is the water flux ( $\text{Lm}^{-2}\text{h}^{-1}$ ),  $\Delta w$  represents the difference in the feed solution weight (g),  $\rho$  is water density at operating temperature (g/L),  $A$  is the actual operative area of the membrane ( $20 \times 10^{-4} \text{ m}^2$ ), and  $t$  is the experiment time.

139 Solute flux through the membrane was estimated by monitoring the conductivity of the feed solution and  
140 using the following equation:

141 
$$J_s = \frac{\Delta CV}{At}$$

142 Where  $J_s$  represents the solute flux ( $\text{gm}^{-2}\text{h}^{-1}$ ),  $\Delta C$  is the change in feed solution concentration (g/L)  
143 (calculated from the conductivity change), and  $V$  stands for the volume of feed solution (L).



144

145 **Figure 2 Schematic diagram of the FO bench-scale test unit.**

### 146 **3. Results and Discussion**

#### 147 **3.1. Membrane characterization**

148 Figure 3 illustrates the SEM captures of PAN's support layer that was prepared by the electrospinning  
149 technique. It can be observed that the membrane structured of smooth and uniform fibers with an  
150 approximate diameter of 250 nm. The cross-sectional SEM image (Figure 4) shows that the membrane  
151 consists of nanofibrous layers with a thickness of about 75 microns. It can also be noticed that the  
152 underlying nanofibers own a very high porosity on their surfaces. This could assure maximum contact  
153 between PAN nanofibers with the draw solution during the forward osmosis operation, which means  
154 higher mass transfer area and consequently higher water flux. Figure 5 illustrates the surface morphology  
155 of the PAN nanofiber membrane after the interfacial polymerization reaction. Also, it can be seen that the  
156 polyamide selective membrane was successfully formed on the PAN nanofiber support sheet. **It can be**

157 seen from the SEM image after the IP reaction that it has a leaf-like morphology compared to the PAN  
158 support layer which has a nanofibrous structure. It was reported in the literature that the leaf-like structure  
159 confirms the formation of the polyamide selective layer. The contact angle measurement of the prepared  
160 membranes showed that it has a hydrophilic surface with an average contact angle of 35°. The  
161 hydrophilicity of the membrane's surface is an important factor in the osmotically driven membrane  
162 processes (Darwish et al., 2020). This could be explained as the solutes can exclusively diffuse within the  
163 wetted area of the support sheet. Ultimately, the unsaturated parts inside the internal structure of the  
164 support layer couldn't be calculated as an actual mass transfer area. As much as the internal surfaces of  
165 the pores and inner vacancy get wet, the porous support layer can contribute to producing a membrane  
166 with a better osmotic water flux performance.

## 167 **3.2. Support sheet mechanical properties and porosity**

### 168 3.2.1 Mechanical properties

169 Using a support layer for the TFC membrane that usually applied in nanofiltration, reverse  
170 osmosis, and forward osmosis is inevitable due to the tiny thickness of the active membrane. The support  
171 layer was found to significantly affect the total performance and commonly made of polymers. Many  
172 factors could influence layer usage such as its raw material, method and conditions of preparation, doping  
173 additives, porosity, tortuosity, etc (Kadhom and Deng, 2018). In most cases, the support layer is  
174 manufactured using the phase inversion phenomenon for a low hydrophilicity polymer. In this work, a  
175 PAN layer was synthesized using the electrospinning, which is expected to produce higher internal  
176 porosity than the sheets produced via phase inversion. Therefore, the mechanical properties were studied  
177 and compared to the commonly used support layer produced by phase inversion.

178 Figure 6 shows the relation between the stress and strain of the PAN sheet. It can observe that the  
179 maximum stress was 1.258 MPa, which was associated with a strain of 15.31%. When these values were  
180 compared with 15% Polyethersulfone support sheet (as an example of the familiarly applied support  
181 layers), the stress is lower but the strain is higher. The measured stress and strain of the PES sheet were  
182 around 2.45 MPa and 8.7%, respectively. It can be noted that the PAN sheets had a lower mechanical



183 strength but a higher elongation rate. This result is expected due to the method of preparation, wherein  
184 the electrospinning the nanofibers are made individually and connect with each other on the rotating  
185 cylinder. While in the phase inversion, the sheet formed by stiffening the polymer and discarding the  
186 solvent. The average values of other mechanical properties were listed in Table 1 with the standard  
187 deviation of three measurement values.

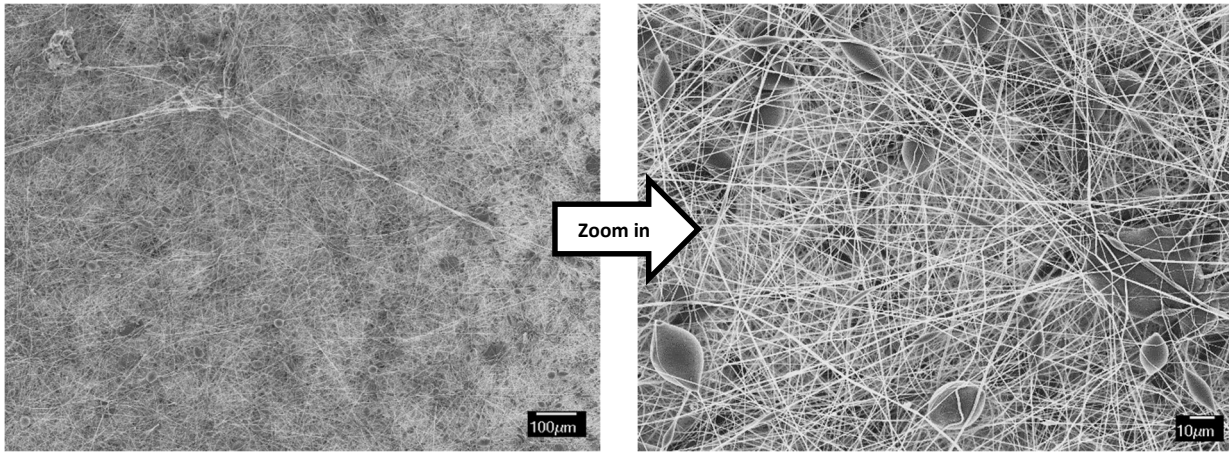
188 **Table 1. Mechanical properties of PAN support layer**

<b>Mechanical Property</b>	<b>Average value</b>	<b>Standard deviation</b>	<b>Units</b>
Young's modulus	9.4065	1.0288	MPa
Tensile strength	1.3586	0.1428	MPa
Elongation at break	17.8463	3.5857	(%)

189

### 190 3.2.2 Porosity

191 PAN support layer was prepared by the electrospinning to achieve a high porosity. However, the  
192 average porosity values of the PAN and classic PES layers were 92.07%  $\pm$ 2.09 and 60.0%  $\pm$ 1.53,  
193 respectively. From these values, it can be seen that the PAN sheet is more porous than the PES sheet.  
194 This could help in penetrating the water and, anyway, solute through the membrane structure, which could  
195 improve the water flux. Higher porosity means lower unreached spaces and dead ends.

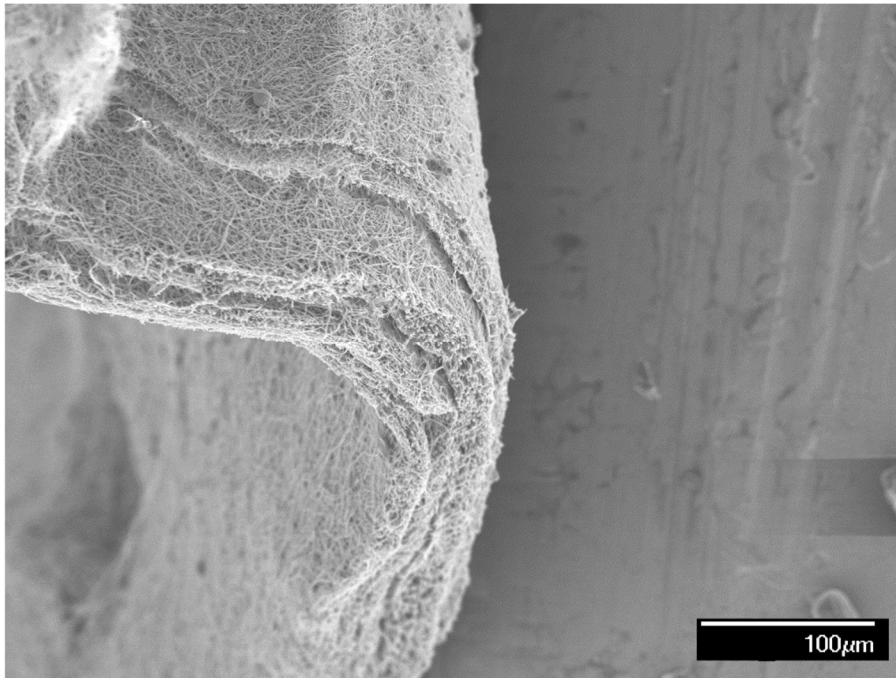


196

197

198

**Figure 3 Surface SEM images of the as-spun PAN nanofiber mat.**



199

200

**Figure 4 Cross-sectional SEM image of the as-spun PAN nanofiber mat.**

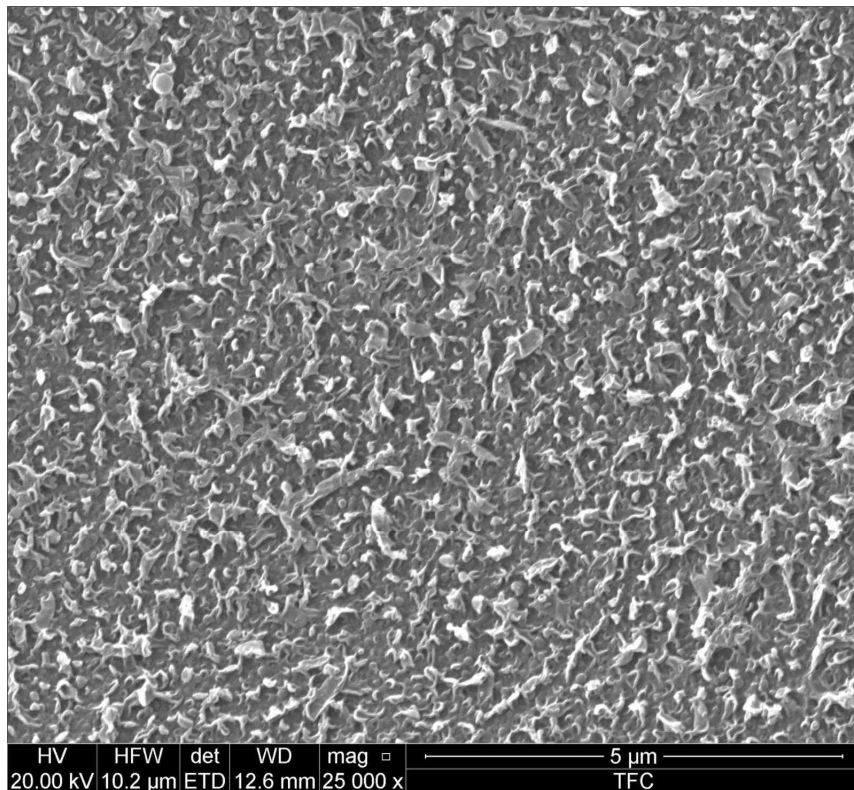
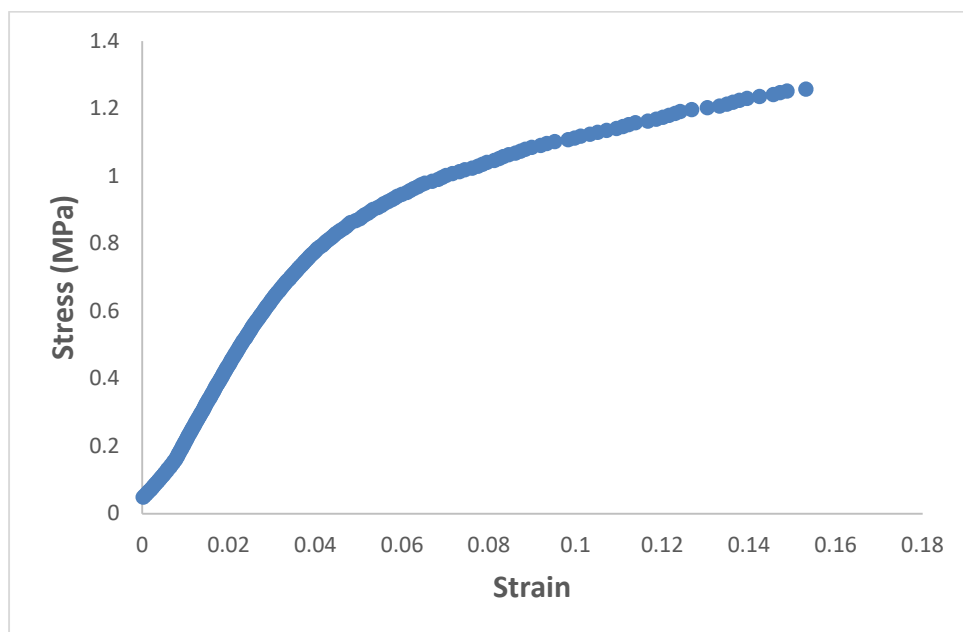
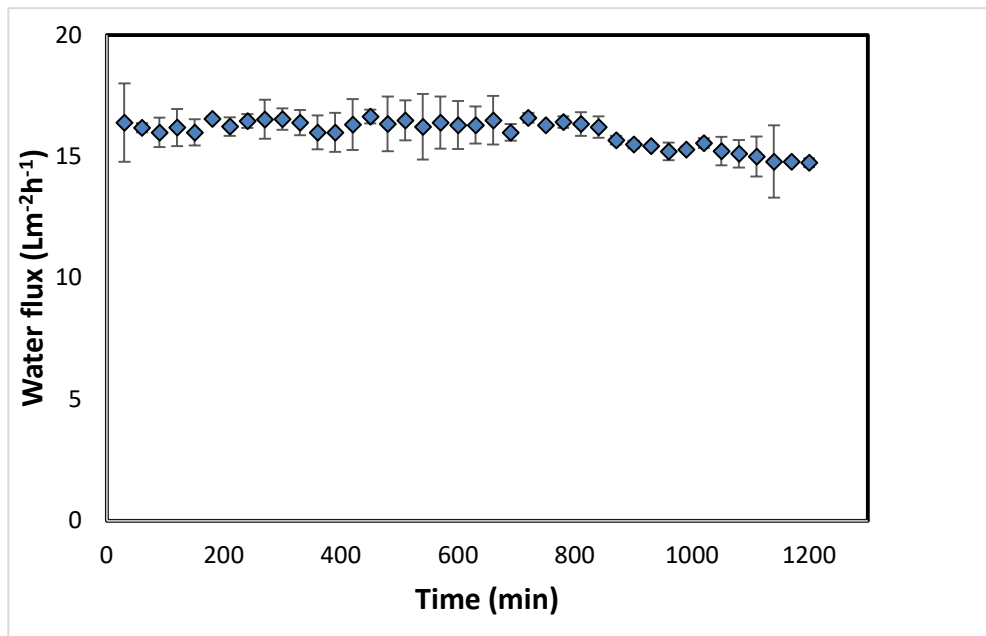


Figure 5 Surface SEM image of the TFC PAN membrane.



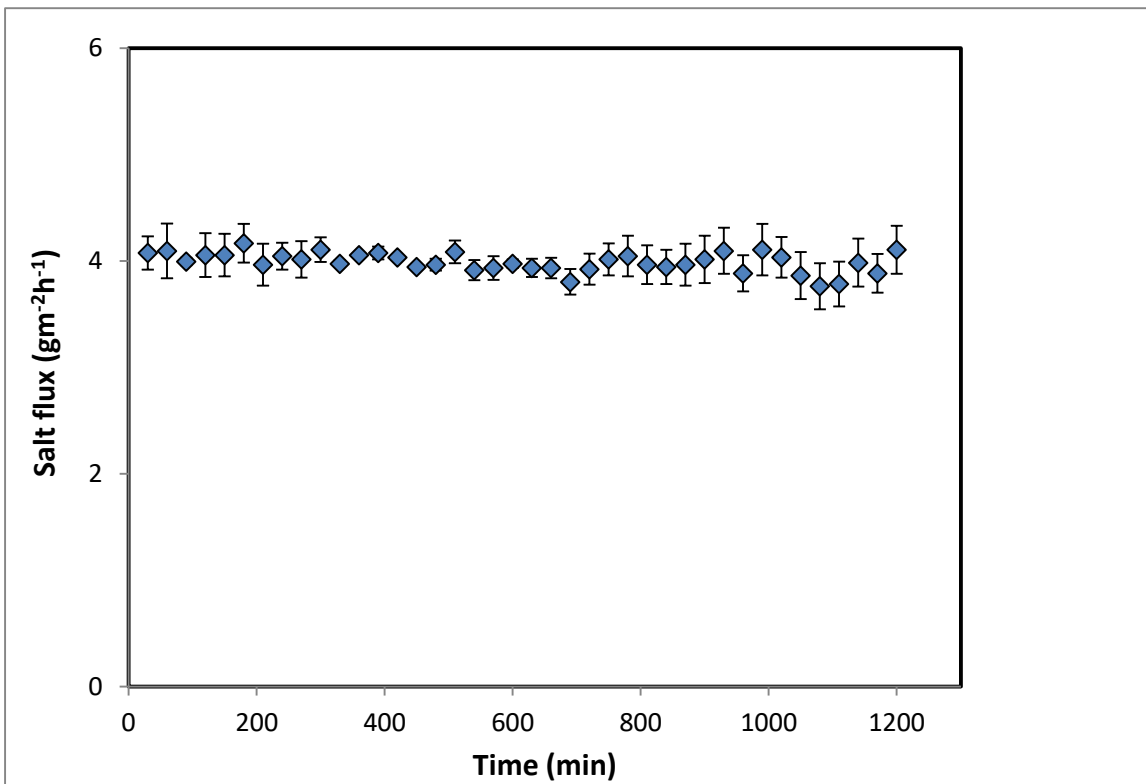
### 204 3.3. Membrane performance in FO operation

205 The osmotic efficiency of the TFC membrane supported by the nanofiber layer was examined using DI  
206 water as a feed solution, whereas 1 M NaCl solution was used as a draw solution according to the  
207 standard methodology for testing the osmotically driven membranes (Cath et al., 2013). Results of water  
208 flux and salt reverse flux are clarified in Figures 7 and 8, respectively. PAN-TFC membrane showed a  
209 stable flux of about 16 LMH for 20 h of operation. Reverse salt flux exhibited similar behavior with an  
210 average value of about 4 GMH. In order to compare the performance of the PAN-TFC membrane with  
211 commercial membranes, we tested CTA membranes from HTI under the same operating conditions, the  
212 results were illustrated in Figure 9. Also, a comparison of the PAN-TFC membrane with some of the  
213 commercially available FO membranes can be found in Table 2. It can be distinguished from the figure  
214 that the PAN-TFC membrane's water flux was higher than the HTI-CTA membrane's water flux. This  
215 could be attributed to the highly porous surface structure of the nanofiber support layer for the PAN-  
216 TFC membrane; this porous surface generates a more effective mass transfer area, and consequently  
217 higher water flux. However, the reverse salt flux of the commercial membrane was lower compared to  
218 the PAN-TFC membrane. This could ascribe to its better mechanical strength and rigidity compared with  
219 the nanofibrous composite membranes, which commonly have modest mechanical properties.  
220 Nevertheless, the FO applications are famous to have low or no hydraulic pressure required to drive the  
221 process; here, it can result that the osmotic efficiency of the membrane is more important than its rigidity.



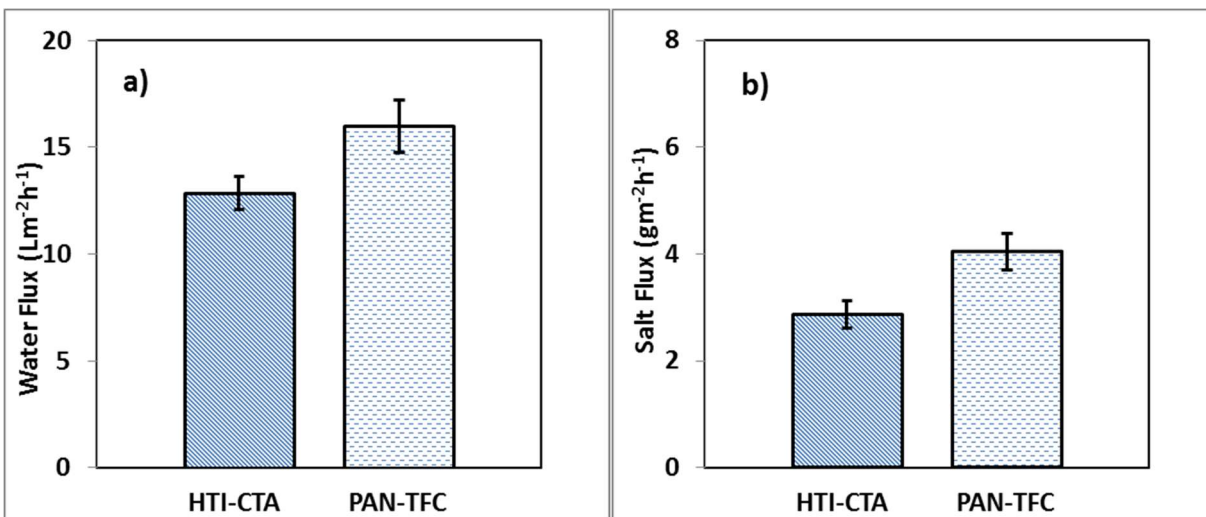
222

223 **Figure 7 Forward osmosis water flux for the PAN-TFC membrane. Experimental conditions: feed solution: DI water,**  
224 **draw solution: 1 M NaCl, FO mode, volumetric flow-rate of feed and draw 0.6 L/min, Temp 25° C, zero transmembrane**  
225 **pressure. Results are an average of three experiments with different coupons. Error bars indicate standard deviation.**



226

227 **Figure 8** Forward osmosis salt flux for the PAN-TFC membrane. Experimental conditions: feed solution: DI water,  
 228 draw solution: 1 M NaCl, FO mode, volumetric flow-rate of feed and draw 0.6 L/min, Temp 25° C, zero transmembrane  
 229 pressure. Results are an average of three experiments with different coupons. Error bars indicate standard deviation.



230

231 **Figure 9 Forward osmosis water flux and salt flux for the PAN-TFC membrane. Experimental conditions: feed**  
232 **solution: DI water, draw solution: 1 M NaCl, FO mode, volumetric flow-rate of feed and draw 0.6 L/min, Temp 25° C,**  
233 **zero transmembrane pressure. Results are an average of three experiments with different coupons. Error bars indicate**  
234 **standard deviation.**

235 **Table 2 Performance of some of the commercially FO membranes.**

Membrane	Feed Solution	Draw Solution	Water Flux	Salt Flux	Reference
PAN-TFC	DI	1 M NaCl	16	4	This work
HTI-TFC	DI	1 M NaCl	15	4.5	(Ren and McCutcheon, 2018)
Aquaporin TFC	DI	1 M NaCl	9	4	(Xia et al., 2017)
Oasys TFC	DI	1 M NaCl	30	50	(Cath et al., 2013)
Porifera CTA	DI	1 M NaCl	29		(Roy et al., 2016)

236

#### 237 **4. Conclusions and Recommendations**

238 TFC membrane with fibrous structure was prepared in this research and tested for forward osmosis  
239 application. The electrospinning setup was made from locally available parts. This system exhibited stable  
240 operation in making the electrospun nanofiber membrane. The prepared TFC membrane showed good  
241 performance in terms of water flux and salt rejection. TFC-PAN membranes showed a stable water flux  
242 with an average value of 16 LMH comparing to the CTA commercial membranes with 13 LMH water  
243 flux. Future research can focus on incorporating specific nanoparticles to enhance membranes'  
244 performance. Also, studying the exposure time of MPD and TMC on the performance of the membrane  
245 is highly recommended.

246

247

248

249 **References**

- 250 Al-Furaiji, M., Benes, N., Nijmeijer, A., McCutcheon, J.R., 2019. Use of a Forward Osmosis–  
251 Membrane Distillation Integrated Process in the Treatment of High-Salinity Oily Wastewater. *Ind.*  
252 *Eng. Chem. Res.* 58, 956–962. <https://doi.org/10.1021/acs.iecr.8b04875>
- 253 Al-Furaiji, M.H.O., Arena, J.T., Chowdhury, M., Benes, N., Nijmeijer, A., McCutcheon, J.R., 2018.  
254 Use of forward osmosis in treatment of hyper-saline water. *Desalin. Water Treat.* 133, 1–9.  
255 <https://doi.org/10.5004/dwt.2018.22851>
- 256 Ang, W.L., Wahab Mohammad, A., Johnson, D., Hilal, N., 2019. Forward osmosis research trends in  
257 desalination and wastewater treatment: A review of research trends over the past decade. *J. Water*  
258 *Process Eng.* 31, 100886. <https://doi.org/10.1016/j.jwpe.2019.100886>
- 259 Bui, N.N., McCutcheon, J.R., 2013. Hydrophilic nanofibers as new supports for thin film composite  
260 membranes for engineered osmosis. *Environ. Sci. Technol.* 47, 1761–1769.  
261 <https://doi.org/10.1021/es304215g>
- 262 Cath, T.Y., Adams, D., Childress, A.E., 2005. Membrane contactor processes for wastewater  
263 reclamation in space: II. Combined direct osmosis, osmotic distillation, and membrane distillation  
264 for treatment of metabolic wastewater. *J. Memb. Sci.* 257, 111–119.  
265 <https://doi.org/10.1016/j.memsci.2004.07.039>
- 266 Cath, T.Y., Childress, A.E., Elimelech, M., 2006. Forward osmosis: Principles, applications, and recent  
267 developments. *J. Memb. Sci.* 281, 70–87. <https://doi.org/10.1016/j.memsci.2006.05.048>
- 268 Cath, T.Y., Elimelech, M., McCutcheon, J.R., McGinnis, R.L., Achilli, A., Anastasio, D., Brady, A.R.,  
269 Childress, A.E., Farr, I. V., Hancock, N.T., Lampi, J., Nghiem, L.D., Xie, M., Yip, N.Y., 2013.  
270 Standard Methodology for Evaluating Membrane Performance in Osmotically Driven Membrane  
271 Processes. *Desalination* 312, 31–38. <https://doi.org/10.1016/j.desal.2012.07.005>
- 272 Chowdhury, M.R., Huang, L., McCutcheon, J.R., 2017. Thin Film Composite Membranes for Forward  
273 Osmosis Supported by Commercial Nanofiber Nonwovens. *Ind. Eng. Chem. Res.* 56, 1057–1063.  
274 <https://doi.org/10.1021/acs.iecr.6b04256>
- 275 Darwish, N. Bin, Alkudhiri, A., AlRomaih, H., Alalawi, A., Leaper, M.C., Hilal, N., 2020. Effect of  
276 lithium chloride additive on forward osmosis membranes performance. *J. Water Process Eng.* 33,



277 101049. <https://doi.org/10.1016/j.jwpe.2019.101049>

278 Huang, L., McCutcheon, J.R., 2014. Hydrophilic nylon 6,6 nanofibers supported thin film composite  
279 membranes for engineered osmosis. *J. Memb. Sci.* 457, 162–169.  
280 <https://doi.org/10.1016/j.memsci.2014.01.040>

281 Kadhom, M., Deng, B., 2019. Synthesis of high-performance thin film composite (TFC) membranes by  
282 controlling the preparation conditions: Technical notes. *J. Water Process Eng.* 30, 100542.  
283 <https://doi.org/10.1016/j.jwpe.2017.12.011>

284 Kadhom, M., Yin, J., Deng, B., 2016. A thin film nanocomposite membrane with MCM-41 silica  
285 nanoparticles for brackish water purification. *Membranes (Basel)*. 6.  
286 <https://doi.org/10.3390/membranes6040050>

287 Linares, R.V., Li, Z., Elimelech, M., Amy, G., Vrouwenvelder, H., 2017. Recent Developments in  
288 Forward Osmosis Processes. *Water Intell. Online*. <https://doi.org/10.2166/9781780408125>

289 McCutcheon, J.R., McGinnis, R.L., Elimelech, M., 2005. A novel ammonia-carbon dioxide forward  
290 (direct) osmosis desalination process. *Desalination* 174, 1–11.  
291 <https://doi.org/10.1016/j.desal.2004.11.002>

292 Ren, J., McCutcheon, J.R., 2018. A new commercial biomimetic hollow fiber membrane for forward  
293 osmosis. *Desalination* 442, 44–50. <https://doi.org/10.1016/j.desal.2018.04.015>

294 Ren, J., McCutcheon, J.R., 2014. A new commercial thin film composite membrane for forward  
295 osmosis. *Desalination* 343, 187–193. <https://doi.org/10.1016/j.desal.2013.11.026>

296 Roy, D., Rahni, M., Pierre, P., Yargeau, V., 2016. Forward osmosis for the concentration and reuse of  
297 process saline wastewater. *Chem. Eng. J.* 287, 277–284. <https://doi.org/10.1016/j.cej.2015.11.012>

298 Waisi, B.I., Manickam, S.S., Benes, N.E., Nijmeijer, A., McCutcheon, J.R., 2019. Activated Carbon  
299 Nanofiber Nonwovens: Improving Strength and Surface Area by Tuning Fabrication Procedure.  
300 *Ind. Eng. Chem. Res.* 58, 4084–4089. <https://doi.org/10.1021/acs.iecr.8b05612>

301 Xia, L., Andersen, M.F., Hélix-Nielsen, C., McCutcheon, J.R., 2017. Novel Commercial Aquaporin  
302 Flat-Sheet Membrane for Forward Osmosis. *Ind. Eng. Chem. Res.* 56, 11919–11925.  
303 <https://doi.org/10.1021/acs.iecr.7b02368>

304

